JOURNAL OF MATERIALS SCIENCE 23 (1988) 3156–3160

Effect of Sn/Sb ratio in determining crystallite size of "SnO_2–Sb_2O_5" semiconductors

G. CARTURAN, P. GIORDANO ORSINI, P. SCARDI
Department of Engineering, University of Trento 38050 Mesiano di Povo, Italy
R. DI MAGGIO
IRST, 38050 Povo, Trento, Italy

Six "SnO_2–Sb_2O_5" semiconductors with different Sn/Sb ratios were prepared by the gel method. The samples, heated at different temperatures in the range 250 to 1100° C, were characterized by X-ray analysis, surface-area determination, TG-DTA studies and SEM observations. Results indicate that the crystallite size of SnO_2 doped by antimony oxide is affected by Sb/Sn ratio, smaller crystallites being obtained at lower antimony oxide loadings. The presence of a Sb_2O_4 phase separated from SnO_2 and the effect of antimony doping on SnO_2 were considered to be the main parameters ruling SnO_2 crystallite dimensions.

1. Introduction

The "SnO_2–Sb_2O_5" semiconductors are well known and extensively studied: these materials are currently exploited for a number of industrial applications, among which is the preparation of semiconducting glaze for insulators of high-power lines [1, 2].

On this topic, some authors have already reported experimental evidence supporting intimate connection between glaze morphology and electrochemical processes responsible for glaze corrosion and collapse of semiconducting properties [3, 4].

More recently, we studied the possible use of the sol–gel process for the production of semiconducting coatings with homogeneous distribution of "SnO_2–Sb_2O_5" solid phase inside the glaze [5]. The common indication of these studies is that small-sized SnO_2 crystallites improve the semiconducting features, also resulting in a better distribution of the semiconducting phase in the entire thickness of the surface layer.

The study of those parameters affecting SnO_2 crystallite size is therefore the primary goal when dealing with "SnO_2–Sb_2O_5" semiconductors set up as films deposited on a bulk ceramic insulator. To this aim, we report here the effect of Sn/Sb ratio on SnO_2 crystallite size starting from the almost amorphous mixture of the two oxides as obtained by the gel method at low temperature. This approach was thought promising even for possible extension of "SnO_2–Sb_2O_5" materials in heterogeneous catalysis where these products were found to behave as effective and valuable catalysts with selectivity features [6].

2. Experimental details

2.1. Materials and instrumentation

Standard techniques for treatment of air-sensitive compounds were thoroughly used during chemical procedures. Solvents were dried by procedures described in the literature [7]. Starting products were commercial analytical reagent grade chemicals.

Scanning electron microscopy (SEM) data were collected using a Cambridge Stereoscan 250 instrument at the CUGAS (University of Padova, Italy). Differential thermal analysis (DTA) and thermogravimetric experiments (TG) were made using a Netzsch STA 409 apparatus. Surface area measurements were performed with a commercial Sorptomatic mod. 1800 Carlo Erba instrument, based on the measurement of the adsorption isotherms of nitrogen. The technique used is of static-volumetric type, according to which the gas volumes adsorbed are calculated by measuring the pressure variation resulting from the adsorption of a portion of a known volume of nitrogen, by the Brunauer–Emmett–Teller (BET) method.

2.2. X-ray diffraction analysis

Powdered samples were examined in reflection mode with a Rigaku D/max-B diffractometer connected with a Casio 6000 personal computer for routine operations, automation and data processing. Cu$K\alpha$ filtered radiation and a proportional detector were employed to scan the range 20 to 70° in 2θ in continuous mode. Each measure was the sum of ten scans corresponding to 16 sec per step of 0.02°. Sample identification was performed by a search–match program supported by JCPDS cards [8]. Fig. 1 shows the 1 1 0 SnO_2 peak for samples at different SnO_2–Sb_2O_5 ratios heated at 1100° C. The good quality of the peak profile allows a reliable application of Scherrer's formula [9] for crystallite-size evaluation.

2.3. Preparation of samples by the gel method

2.3.1. Synthesis of SnO_2–Sb_2O_5 (99/1)

$SnCl_4$ (7.95 ml) and $SbCl_5$ (0.09 ml) were reacted at −80° C with 30 ml dry CH_3OH. HCl was evolved. 1 ml H_2O was added to this solution. Solvent was eliminated by slow evaporation under vacuum

0022–2461/88 $03.00 + .12

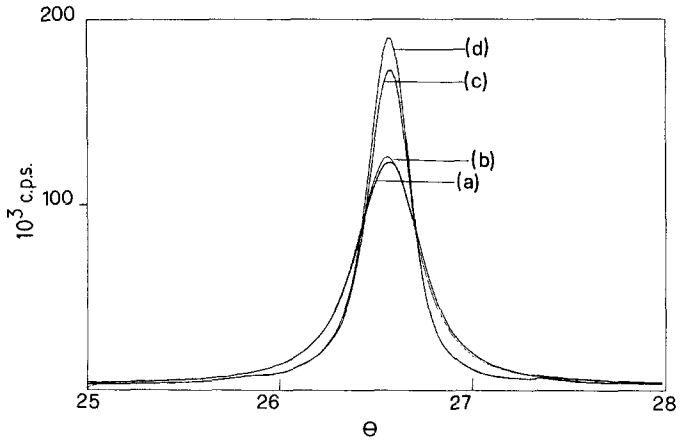

Figure 1 1 1 0 SnO_2 peak for samples heated at 1100° C for different SnO_2/Sb_2O_5 weight ratios: (a) = 99/1, (b) = 98/2, (c) = 95/5, (d) = 90/10.

(10^{-3} torr) affording a gel. This was dried at 170° C for 4 h to remove residual solvent. The product, divided into four parts, was heated at 250, 550, 800, 1100° C, respectively, using a heating rate of 4° C min^{-1}.

Synthesis of SnO_2–Sb_2O_5 (98/2), (97/3), (95/5), (90/10), (85/15) gels was performed using the same procedure reported for the above sample, starting from appropriate amounts of $SnCl_4$ and $SbCl_5$.

3. Results

The Sb(V)/Sn(IV) atomic ratio in "SnO_2–Sb_2O_5" industrial semiconductors falls in the range 2 to 35/100. Thus, we restrict our study to gel samples having SnO_2–Sb_2O_5 weight ratios = 99/1, 98/2, 97/3, 95/5, 90/10 and 85/15.

Preparation details for the synthesis of an individual specimen by the sol–gel process are reported in Section 2; working conditions and handling are analogous to those reported in the previous work [5] except that less severe oxidizing environments are adopted here.

Chemical and morphological evolutions on heating are followed by analysis of specimens treated at 250, 550, 800 and 1100° C for each sample. X-ray spectra indicate that all xerogels at 250° C are microcrystalline or better sub-crystalline SnO_2-based materials.

Progressive heating leads to SnO_2 crystallite size increase, followed by separation of Sb_2O_5 phase, observed by X-ray analysis for samples heated above 800° C. Fig. 2 shows this behaviour in the case of 95/5 = SnO_2–Sb_2O_5 sample: SnO_2 microcrystals are extant even at 250° C; their size grows with temperature increase to give a well-detectable crystallized SnO_2-cassiterite phase. The low concentration of Sb(V) in most samples does not allow an accurate description based on reliable X-ray analysis either of Sb(V)/Sb(III) reduction either of Sb_2O_4 crystallization and separation.

The size of SnO_2 crystallites is evaluated using the approximation of Scherrer's formula [9] which appears suitable considering the restricted range of SnO_2 crystallites size (50 nm) and the expected absence of microscopical stresses for materials obtained by our crystallization procedure. The upper size limit of about 50 nm for SnO_2 crystallites of samples heated at 1100° C is confirmed by several SEM observations. Fig. 3 shows a typical micrograph: SnO_2 crystallites are collected in sponge-like aggregates, individual crystallite size being at the limit of instrumental magnification power i.e. 20 nm. The picture shows the presence of a minor amount of well-shaped crystals which result from microprobe analysis, to be constituted by pure antimony oxide. On the other hand, our primary purpose is to find a reliable tool for crystallite size comparison of powders with different Sn/Sb ratios. Table I gives the SnO_2 average crystallites size resulting from X-ray analysis and subsequent data treatments, for samples treated under identical experimental conditions at 1100° C. It is evident that as the antimony oxide content exceeds 3%, the SnO_2 crystallite dimensions rise from about 25 nm to about 45 nm, thereby suggesting that chemical composition

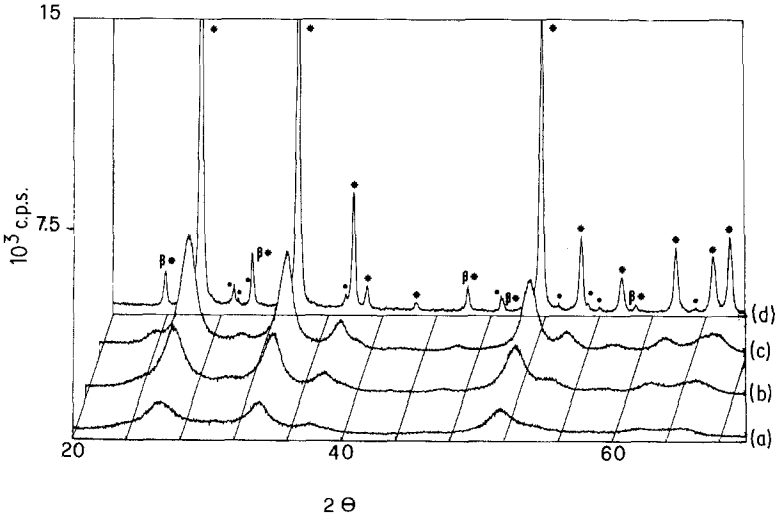

Figure 2 SnO_2 crystallization on heating: (a) = 250° C, (b) = 550° C, (c) = 800° C, (d) = 1100° C for SnO_2/Sb_2O_5 = 95/5 sample. (∗) SnO_2, (•) Sb_2O_4.

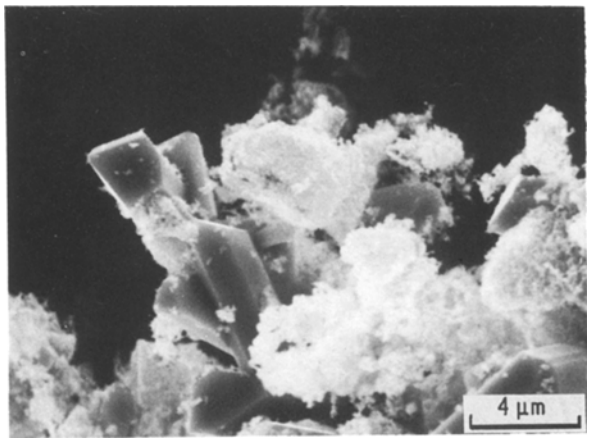

Figure 3 Scanning electron micrograph of SnO_2/Sb_2O_4; well-shaped large crystals are identified as Sb_2O_4.

affects the morphology of SnO_2 phase. X-ray analysis data give only qualitative information on the presence of Sb_2O_4.

The crystallization of gels is also followed by measuring the change of specific surface area as a function of thermal treatment and composition. Fig. 4 shows the typical behaviour describing the effect of heating on surface area reduction: crude xerogel is involved by a progressive lowering of surface development from an initial value of about $180\,m^2\,g^{-1}$ to $16\,m^2\,g^{-1}$ for a sample heated at 1100° C. This trend is observed in all cases; the specific surface area of products treated at 1100° C falls in the range 10 to $30\,m^2\,g^{-1}$, confirming small particle dimensions and the suitability of the preparation procedure for the achievement of large surface area "SnO_2–Sb_2O_5" materials. Thermal analyses recorded for all samples do not give conclusive evidence about the temperature of nucleation and crystallization. In fact, DTA and TG data do not show definite peaks attributable to individual phase separations (Fig. 5). Observed weight loss is assigned to solvent and organic by-product release and/or oxidation; the latter reaction is presumably responsible for the large exothermal range below 400° C.

TABLE I The SnO_2 average crystallite size of samples treated at 1100° C

Weight ratios SnO_2/Sb_2O_5	Crystallite size (nm)*
85–15	42 (43)
90–10	42 (46)
95–5	40 (42)
97–3	25 (27)
98–2	25 (26)
99–1	23 (25)

*The values refer to 1 1 0 SnO_2 peak; data in parentheses refer to 2 0 0 SnO_2 peak.

4. Discussion

X-ray, DTA, SEM and surface analysis data show that the general features of "SnO_2–Sb_2O_5" semiconductors prepared here are substantially identical for all samples, irrespective of chemical composition. The starting products (xerogels heated at 250° C) are already constituted by SnO_2 crystallites smaller than 5 nm without detectable presence of non-crystalline phase; indeed, no haloes at low 2θ are observed by X-ray analysis. These nuclei increase progressively in size affording at 1100° C as well-formed SnO_2 crystals doped by antimony oxides: just above 550° C all samples appear blue in colour, confirming the effective doping of SnO_2 by antimony oxide with the occurrence of semiconducting features [10]. The chemical procedure used for the preparation of the xerogels does not result in the formation of really amorphous materials: thus, it is not surprising that the evolution of most physical properties on heating differs from the case of SiO_2-based gels. For instance, the large surface area of ordinary gels disappears completely upon thermal treatment above 400° C, owing to pore shrinkage and progressive collapsing to glass density [11–13]. The "SnO_2–Sb_2O_5" materials studied here are given, by the thermal treatment, a progressive increase of crystal sizes from an already microcrystalline material; accordingly, specific surface area decreases to a limited extent and final products maintain considerable surface areas even at 1100° C. This fact is confirmed by reported SEM observations. On the

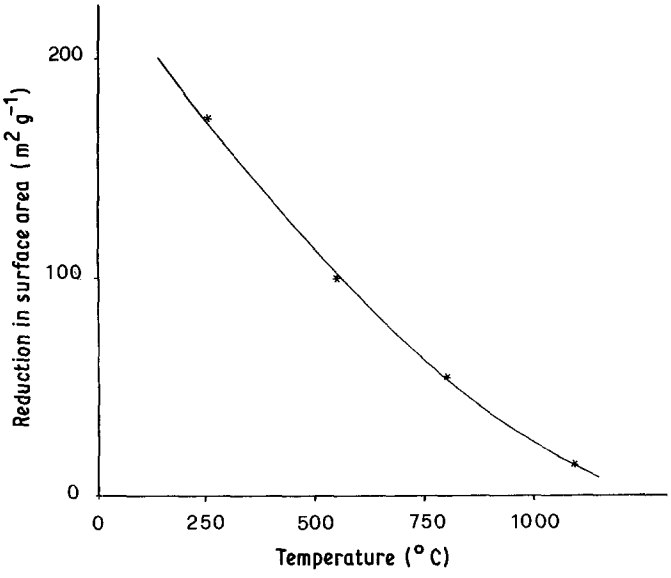

Figure 4 Surface area reduction with temperature. Sample SnO_2/Sb_2O_5 = 98/2.

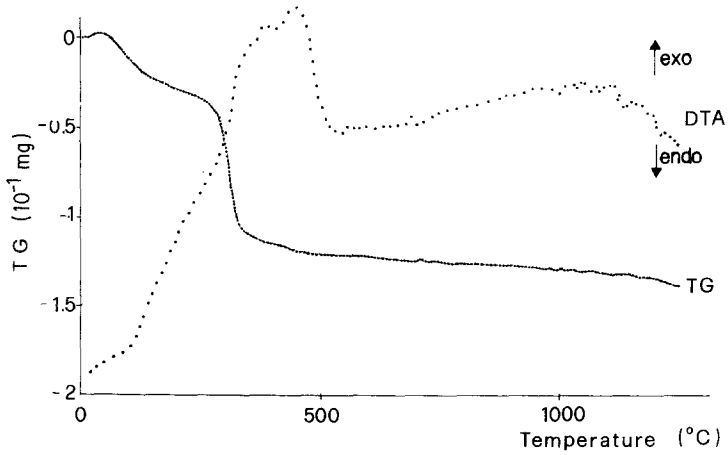

Figure 5 DTA and TG data for SnO_2/Sb_2O_5 = 95/5 sample.

other hand, the lack of definite crystallization peaks in DTA diagrams agrees and confirms the absence of a precise crystallization from an amorphous phase.

This fact constitutes valuable improvement in comparison with previous work where the "SnO_2–Sb_2O_5" semiconducting phase was extracted from xerogels holding massive non-crystalline material; in that case crystallization nuclei, once formed, are capable of continuous growth at the expense of residual amorphous phase, affording coarse-shaped SnO_2 phase with individual crystalline dimensions above 200 nm. In the present work, this upper limit was found from some samples to be about one order of magnitude less (Table I).

For the antimony oxide phase observed here as Sb_2O_4, the non-oxiding preparation environment during the synthesis may be invoked to account for the absence of Sb_2O_5 found in the previous work. This fact can assure a better stability on reduction of high temperatures where a sudden reduction of unstable Sb_2O_5 may result in a swift general collapse of both tin and antimony oxides to metallic phases [5].

In the hypothesis that semiconducting features arise from the defective influence of antimony loading on SnO_2 crystallites, one should expect an improvement of semiconducting ability per unit of mass in case of largely defective and small SnO_2 crystallites. For SnO_2 cassiterite it seems obvious that antimony oxide content should be limited by flexibility of the SnO_2 cell in the cassiterite lattice, so that bigger crystals are expected for poorly doped materials. On the other hand, the simultaneous occurrence of Sb_2O_4 phase separation during SnO_2 crystal growth may promote Sb(III) or Sb(V) extraction from doped SnO_2 crystallites.

SnO_2 crystallite size depends on the percentage of oxide and Fig. 6 shows the observed trend of SnO_2 average crystallite size for samples at 1100° C as a function of nominal Sb_2O_5 content; the dimensions of the crystallites suddenly increase from ~25 to ~50 nm as the nominal antimony oxide content exceeds 3%. The interpretation of this result agrees with the above considerations: the simultaneous SnO_2 crystallite growth and Sb_2O_4 phase separation are quenched at low antimony oxide contents. On the other hand, high antimony oxide loadings allow a better Sb_2O_4 phase crystallization even reducing the defective presence of antimony into SnO_2, so that it can crystallize better affording larger crystallites. In conclusion, the use of low percentages of antimony, while assuring the "SnO_2–Sb_2O_5" semiconductors performance, presents the advantage of a limited extension in SnO_2 crystallite size which can be better dispersed into a glass-phase coating for electrical insulators.

Acknowledgement

Financial support for the present work was provided by M.P.I. (40% found) Rome.

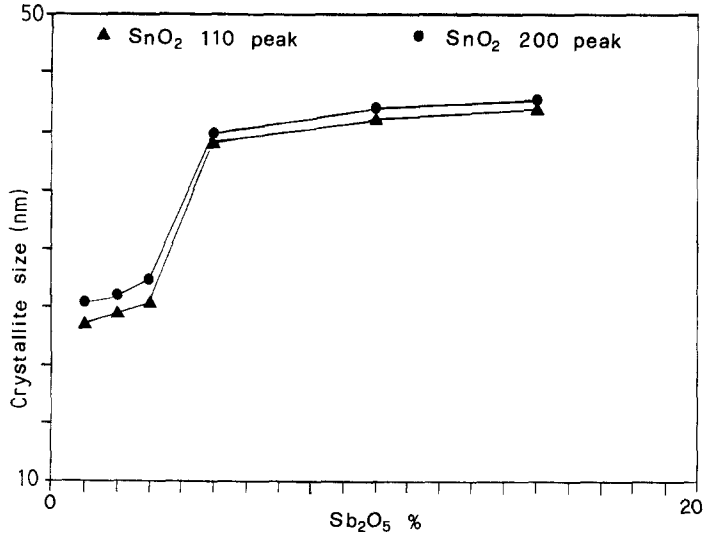

Figure 6 Average crystallite size plotted against Sb_2O_5 content. (▲) SnO_2 1 1 0 peak, (●) SnO_2 2 0 0 peak.

References

1. P. J. LAMBERT, *Proc. IEE* **118** (1971) 1107.
2. D. B. BINNS, *Trans. Brit. Ceram. Soc.* **73** (1974) 7.
3. D. G. POWELL, *Amer. Ceram. Soc. Bull.* **25** (1973) 600.
4. G. BAGNASCO, P. PERNICE and P. G. ORSINI, *Ceram. Int.* **5** (1979) 161.
5. G. COCCO, S. ENZO, G. CARTURAN, P. G. ORSINI and P. SCARDI, *Mater. Chem. Phys.* **17** (1987) 541.
6. G. CENTI and F. TRIFIRO', *Catal. Rev. Sci. Engng* **28** (1986) 165.
7. D. D. PENIN, W. L. F. ARMAREGO and D. R. PENIN, "Purification of Laboratory Chemicals" (Pergamon, Oxford, U.K., 1966).
8. JCPDS, International Center of diffraction Data, 1605, Park Lane, Swarthmore, Pennsylvania, USA.
9. H. P. KLUG and L. E. ALEXANDER, "X-ray Diffraction Procedures", 2nd Edn. (Wiley, New York, 1974).
10. R. H. TAYLOR, D. L. ALLISON and T. I. BARRY, *J. Mater. Sci.* **13** (1978) 876.
11. G. CARTURAN, V. GOTTARDI and M. GRAZIANI, *J. Non-Cryst. Solids* **29** (1978) 41.
12. G. CARTURAN, G. COCCO, L. SCHIFFINI and G. STRUKUL, *J. Catal.* **65** (1980) 359.
13. G. CARTURAN, G. FACCHINI, V. GOTTARDI and G. NAVAZIO, *J. Non-Cryst. Solids* **63** (1974) 273.

Received 17 July 1987
and accepted 15 January 1988